

Self-propelled sweeping removal of dropwise condensate

Xiaopeng Qu,¹ Jonathan B. Boreyko,^{2,3} Fangjie Liu,¹ Rebecca L. Agapov,² Nickolay V. Lavrik,² Scott T. Retterer,² James J. Feng,^{4,5} C. Patrick Collier,² and Chuan-Hua Chen^{1,a)}

¹*Department of Mechanical Engineering and Materials Science, Duke University, Durham, North Carolina 27708, USA*

²*Center for Nanophase Materials Sciences, Oak Ridge National Laboratory, Oak Ridge, Tennessee 37831, USA*

³*Bredesen Center for Interdisciplinary Research, University of Tennessee, Knoxville, Tennessee 37996, USA*

⁴*Department of Mathematics, University of British Columbia, Vancouver, British Columbia V6T 1Z2, Canada*

⁵*Department of Chemical and Biological Engineering, University of British Columbia, Vancouver, British Columbia V6T 1Z3, Canada*

(Received 30 November 2014; accepted 20 May 2015; published online 2 June 2015)

Dropwise condensation can be enhanced by superhydrophobic surfaces on which the condensate drops spontaneously jump upon coalescence. However, the self-propelled jumping in prior reports is mostly perpendicular to the substrate. Here, we propose a substrate design with regularly spaced micropillars. Coalescence on the sidewalls of the micropillars leads to self-propelled jumping in a direction nearly orthogonal to the pillars and therefore parallel to the substrate. This in-plane motion in turn produces sweeping removal of multiple neighboring drops. The spontaneous sweeping mechanism may greatly enhance dropwise condensation in a self-sustained manner. © 2015 AIP Publishing LLC. [<http://dx.doi.org/10.1063/1.4921923>]

Dropwise condensation is known to be significantly more effective than its filmwise counterpart in terms of phase-change heat transfer.^{1–3} The effectiveness stems from the rapid removal of the liquid condensate, whose poor thermal conductance hinders condensation heat transfer. In conventional dropwise condensation on a hydrophobic (lyophobic) surface, the rapid removal is largely due to the sweeping removal of groups of condensate drops, typically by gravity.^{2,3} The sweeping removal leaves bare areas for renucleation followed by the early-stage growth of small condensate drops, giving rise to effective thermal transport. Despite its convenience and widespread use, the gravitational removal mechanism is orientation dependent and only effective for drop sizes approaching the millimetric capillary length.⁴

To alleviate the dependence on external forces including gravity and shear, alternative mechanisms have been proposed to augment condensation heat transfer by exploiting the intrinsic surface energy.^{5–7} These mechanisms induce capillary flow by manipulating the surface tension of the working fluid, the wettability of the substrate, and/or the geometry of the surface texture.^{8–18} Among them, completely passive mechanisms are usually slow in transporting condensate because the driving surface tension is balanced by viscous stresses, either along the contact line of condensate drops or on the walls of wicking tracks. Although friction can be reduced by surface textures that trap air or liquid lubricants,^{19,20} such techniques need to be used in conjunction with an effective removal mechanism to achieve high transport speed. As an alternative to the capillary-viscous mechanism, capillary-inertial processes can remove small condensate drops rapidly and spontaneously.^{21–23} Indeed,

condensate drops are known to spontaneously jump at a high speed upon coalescence on superhydrophobic (superlyophobic) surfaces,^{21,22} and the self-propelled jumping has been demonstrated to augment condensation heat transfer.^{24–26} However, the self-propelled jumping reported so far is mostly perpendicular to the textured substrate. The out-of-plane directionality is not conducive to the sweeping removal of neighboring drops, a potential mechanism to significantly enhance dropwise condensation in a self-sustained manner.

Here, we report the integration of the sweeping removal with the self-propelled motion on a textured substrate. In contrast to prior reports where the coalescence-induced jumping motion is out of plane and essentially perpendicular to the substrate, the surface textures are designed to facilitate spontaneous motion that is in plane and mostly parallel to the substrate. The key idea to enable the in-plane motion is schematically shown in Fig. 1. Condensate drops within the

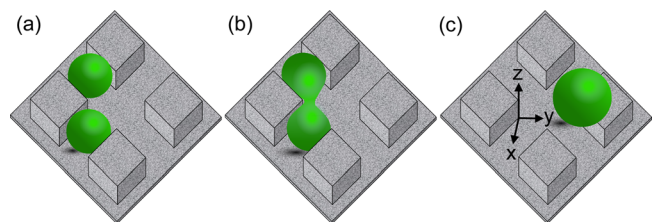


FIG. 1. Schematic of the pillared surface facilitating the sweeping removal. (a) Two condensate drops nucleate and grow within the forest of micropillars. (b) The drops grow to a large enough size to coalesce around the corner of a pillar. (c) The merged drop jumps in a direction nearly orthogonal to the sidewalls of the pillar, and therefore parallel to the substrate. The slight upward motion is due to the presence of the bottom substrate supporting the pillars. A coordinate system is attached to the bottom corner of the pillar of interest, with y along the symmetry line (the primary direction of the jumping motion) and z perpendicular to the substrate in the xy plane.

^{a)}chuanhua.chen@duke.edu

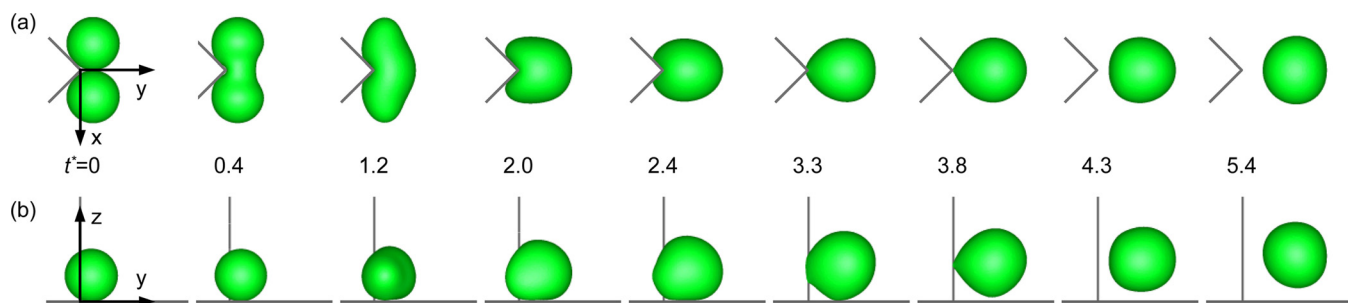


FIG. 2. Simulated coalescence process on the sidewalls of a non-wetting pillar supported by a non-wetting substrate, as sketched in Fig. 1: (a) top xy view; (b) side yz view. The Ohnesorge number is 0.0398. The time stamps are nondimensionalized by the capillary-inertial time (t_{ci}), which is $3.71 \mu\text{s}$ for drops of $10 \mu\text{m}$ radius. The departure from the bottom substrate and pillar sidewalls occurs around $t^* = 3.3$ and 3.8 , respectively. (Multimedia view) [URL: <http://dx.doi.org/10.1063/1.4921923.1>] [URL: <http://dx.doi.org/10.1063/1.4921923.2>] [URL: <http://dx.doi.org/10.1063/1.4921923.3>]

forest of micropillars merge and jump nearly orthogonally to the sidewalls of the vertical micropillars, giving rise to a self-propelled motion essentially parallel to the substrate.

In Fig. 2 (Multimedia view), the coalescence process depicted in Fig. 1 is numerically simulated to show the self-propelled motion conducive to the sweeping removal. All solid surfaces are non-wetting with a contact angle of 180° . As in Fig. 1(b), the coalescing drops are identical in size and initially tangent to the two orthogonal sidewalls of the pillar as well as the bottom substrate. Except for the different geometry adopted here, the numerical procedures follow that used in Liu *et al.*^{27,28} The fluid properties correspond to water and air at 20°C . The governing parameter is the Ohnesorge number, $Oh = \mu_L / \sqrt{\rho_L \sigma r_0}$, where μ_L is the liquid viscosity, ρ_L is the liquid density, σ is the liquid-gas surface tension, and r_0 is the initial radius of the drops prior to coalescence. In Fig. 2, $Oh = 0.0398$ which corresponds to a water drop with a radius of $10 \mu\text{m}$. The self-propelled process in Fig. 2 is representative of all low-Ohnesorge-number cases ($Oh \lesssim 0.1$), which is governed by the capillary-inertial velocity ($u_{ci} = \sqrt{\sigma / \rho_L r_0}$) and time ($t_{ci} = \sqrt{\rho_L r_0^3 / \sigma}$).²⁷

In the top-view Fig. 2(a), the jumping process from a cornered non-wetting pillar resembles that from a flat non-wetting substrate in Liu *et al.*²⁷ The pillar forces the liquid mass that would have expanded past it to move in the opposite direction, leading to a self-propelled motion. Compared to a flat surface, the pillar interferes with the coalescence process at an earlier stage since the cornered surface is closer to the point of coalescence. Consequently, a higher departure velocity is expected in the y -direction. Indeed, the departure velocity orthogonal to the pillar is $v_y^* = v_y / u_{ci} = 0.34$, which is larger than the nondimensional departure velocity of 0.23 on a flat substrate.²⁹ Note that the departure velocity here is measured at the point when the merged drop leaves the surface of interest.

The side-view Fig. 2(b) illustrates another important feature for the sweeping removal, the slight upward velocity, without which the in-plane motion would just lead to back-and-forth bouncing within the four-pillar cell shown in Fig. 1. This upward motion is due to the bottom substrate. The three-dimensional (3D) drop coalescence process is bounded by not only the sidewalls of the pillar but also the bottom substrate. In fact, the bottom substrate interferes with the drop coalescence in essentially the same manner as that in conventional

jumping drops on a flat substrate. Indeed, the vertical departure velocity $v_z^* = 0.19$ is close to the nondimensional velocity of 0.23 on flat superhydrophobic substrates.

To implement the micropillared structures in Fig. 1 for the sweeping removal, the surface wettability needs to be carefully designed. When the microstructures are non-wetting (approaching 180°), tiny condensate drops will coalesce and jump prematurely in a direction orthogonal to any local surface (e.g., the bottom of the substrate), at a size much smaller than the inter-pillar separation. Such premature jumping follows the same out-of-plane jumping mechanism as in prior reports²² and is not conducive to the sweeping motion that requires a consistent and significant in-plane velocity component. On the other hand, the surface coating must be hydrophobic enough (above 90°), otherwise the condensate drops will completely wet the interstitial spaces of the microstructures,¹⁰ forfeiting any self-propelled motion. Below, we offer one of the many possible ways to realize the sweeping idea conveyed in Fig. 1. Our design in Fig. 3 features a two-tier surface morphology, with a nanoroughness coating effectively producing the intermediate hydrophobicity for the micropillars.

The substrate with two-tier roughness was prepared by conformally covering silicon micropillars with aluminum

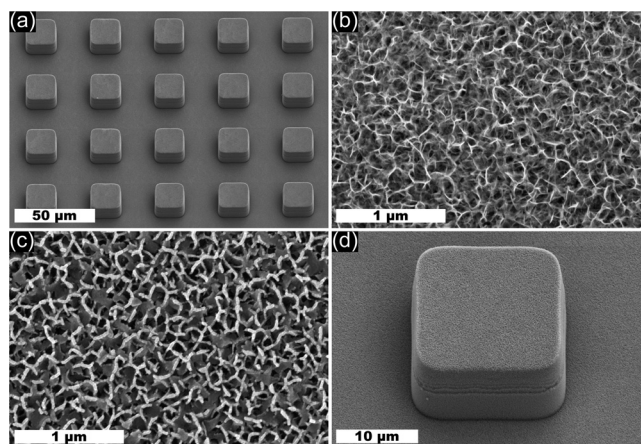


FIG. 3. Two-tier roughness with silicon microstructures conformally coated by aluminum nanostructures: (a) micropillar array etched in silicon; (b) aluminum hydroxide nanostructures on a 100 nm -thick aluminium film, immediately after the hydrothermal reaction; (c) coarsened nanostructures after coating with a 10 nm layer of gold; (d) micropillared surface with a conformal coating of nanostructures shown in (c).

nanostructures (Fig. 3). The micropillars shown in Fig. 3(a) were lithographically etched in a silicon substrate using cryogenic reactive ion etching at -110°C (Oxford Plasmalab 100). The squarely arranged micropillars were designed to have cross section of $20\ \mu\text{m} \times 20\ \mu\text{m}$ and an edge-to-edge separation of $20\ \mu\text{m}$. The pillar height was $10\ \mu\text{m}$ by controlling the etching time. The microstructures were coated with a $100\ \text{nm}$ layer of aluminum using an electron beam evaporator (Thermionics VE-240). A conformal coating was obtained by holding the wafer at a 45° angle and rotating at $20\ \text{rpm}$ during aluminum deposition. The wafer was subsequently immersed in a bath of deionized water heated to 70°C for $10\ \text{min}$, and the hydrothermal reaction generated the aluminum hydroxide nanostructure^{30,31} shown in Fig. 3(b). The two-tier structure was then sputtered with a $10\ \text{nm}$ -layer of gold (Denton Desk IV), and coated with a monolayer of 1-hexadecanethiol (Acros AC12052-0100). Note that the $10\ \text{nm}$ -thick coating actually altered the fine aluminum nanostructure, evident by the contrast between the new nanostructures in Fig. 3(c) compared to Fig. 3(b). Therefore, the $10\ \text{nm}$ thickness of the gold layer was an important parameter for the two-tier texture shown in Fig. 3(d) and used below. The apparent contact angle of the nano-tier-only roughness with alkylthiol coating in Fig. 3(c) was measured to be $161 \pm 3^{\circ}$ (advancing) and $135 \pm 3^{\circ}$ (receding).

During the condensation experiments, the substrate was cooled to 3°C by a recirculating chiller (Thermo Scientific Accel-250LC) through a cold plate. The ambient air was at 22°C with a relative humidity of 45% , corresponding to a dew point of 9.5°C . The supersaturation at the substrate surface was calculated as 1.6 .³² The condensation process on the horizontal, upward-facing substrate was visualized by an optical microscope (Nikon Eclipse LV150) with a $10\times$ lens, and recorded by a high-speed camera (Phantom v710). With the specific two-tier structure shown in Fig. 3(d), the condensation typically nucleated from between the pillars, where the cornered surfaces with an wedge angle below 180° could in principle lower the barrier for heterogeneous nucleation.³³ (The preferential condensation could also arise from defects in the surface coating.^{14,34}) Constrained by the patterned micropillars, the growing drops merged together to form

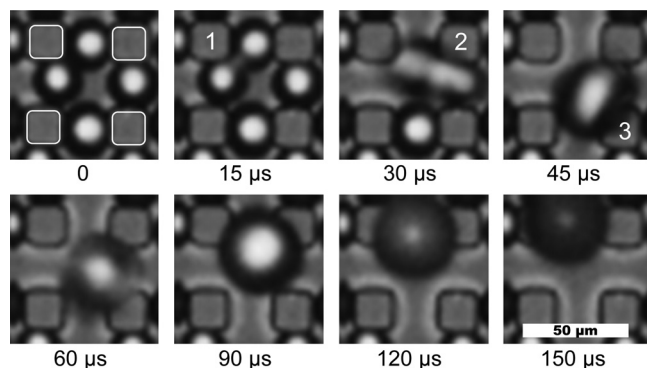


FIG. 4. Coalescence of condensate drops within a cell of four pillars (white squares). The coalescence around pillar 1 triggered subsequent coalescences around pillars 2 and 3 (1st row), leading to the departure of a merged drop from the cell (2nd row). In addition to a significant in-plane velocity, the merged drop had an appreciable velocity component out of plane, apparent from the increasingly blurry images. (Multimedia view) [URL: <http://dx.doi.org/10.1063/1.4921923.4>]

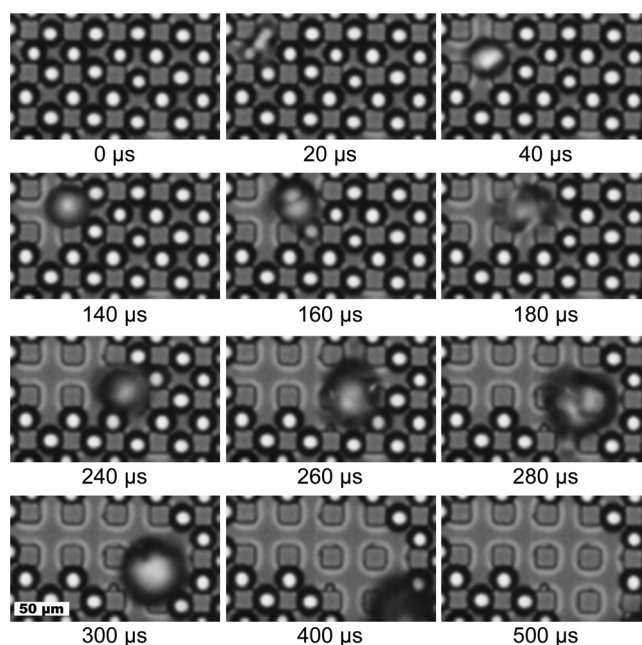


FIG. 5. Chain removal triggered by drop coalescence around the top left pillar. The merged drop from the associated four-pillar cell departed with a significant in-plane velocity (1st row). Subsequent coalescences with neighboring drops gave rise to a chain of coalescence events (2nd-4th rows), removing a total of 15 condensate drops. (Multimedia view) [URL: <http://dx.doi.org/10.1063/1.4921923.5>]

larger drops that were regularly positioned. When the drop radii grew to be comparable to the inter-pillar separation, some neighboring drops coalesced to trigger the spontaneous departure from the substrate, as shown in Figs. 4 and 5. Note that coalescing drops did not spontaneously jump in the absence of the micropillars. On a control substrate with only the alkylthiol-coated nanoroughness in Fig. 3(c), there was no self-propelled motion.

A series of drop coalescences within a four-pillar cell are shown in Fig. 4 (Multimedia view). The initial coalescence was triggered by growing condensate drops around pillar 1, as sketched in Fig. 1. The merged drop moved orthogonally to pillar 1, coalescing with another drop around pillar 2. The oscillation and movement of the newly merged drop caused yet another coalescence around pillar 3. After this series of coalescence, all four drops within the cell were eventually absorbed into one large drop, which departed with significant velocities both in plane (v_x and v_y) and out of plane (v_z).

The self-removal process in Fig. 4 is well predicted by the 3D simulation in Fig. 2. The time scale for drop sweeping is accurately captured. In Fig. 2, the departure from the pillar occurs at $t^* = 3.8$, corresponding to a dimensional time of $14\ \mu\text{s}$. In Fig. 4, a coalescence event occurred every $15\ \mu\text{s}$ or so. The slanted departure in Fig. 4 is consistent with the simulated initial coalescence in Fig. 2, which shows the role of both the pillar sidewalls and bottom substrate in imparting to the merged drop a momentum perpendicular to the respective surfaces. Since the height of the micropillars was comparable to the inter-pillar separation, the predominantly in-plane motion shown in Fig. 2 favored the series of coalescence in Fig. 4 instead of a direct out-of-plane jumping upon the initial coalescence. Note that the condensate drops of the first coalescence were probably situated differently

from Fig. 2. For example, the drops did not need to be in initial contact with the bottom substrate for it to impart an out-of-plane momentum.²⁸ A limitation of the simulation is the 180° contact angle assumed in Fig. 2. More realistic simulations should account for the finite drop-substrate adhesion as well as the contact angle hysteresis.

Building on the four-pillar cell in Fig. 4, we demonstrated the chain removal of a large number of drops in Fig. 5 (Multimedia view). The sweeping motion was triggered by the initial coalescence around the top left pillar, where two growing drops merged on the adjacent sides. The merged drop launched away nearly orthogonally to the vertical pillar (parallel to the substrate). The in-plane motion triggered a chain of coalescence events that picked up a large number of drops along the sweeping path of the merged drop, which grew in size as new drops were absorbed. The sweeping motion left a dry path for renucleation followed by early-stage growth, known to promote effective condensation heat transfer. The merged drop was also moving slightly out of plane (and therefore out of focus), as simulated in Fig. 2 and confirmed in Fig. 4. The out-of-plane motion helped the merged drop to climb out of the initial four-pillar cell to sweepingly remove additional drops. It should be stressed that gravity was playing a negligible role in the sweeping removal powered by surface energy, particularly for the condensate drops with a radius of only around 10 μm. For the entire duration of 500 μs in Fig. 5, gravity could vertically displace a droplet initially at rest by only 1 μm, negligible compared to the drop size and pillar height. Note that Fig. 5 differs from prior reports of multiple-drop removal^{13–15} in that the sweeping removal is triggered by in-plane motion in a completely self-propelled manner.

In summary, we have demonstrated the self-propelled sweeping removal of condensate drops on micropillared surfaces. The sweeping removal hinges on the generation of in-plane motion by inducing self-propelled motion that is nearly orthogonal to the vertical micropillars. Although the proof of concept has been realized using a micropillared surface with nanoroughness coating, the self-propelled sweeping concept is not restricted to such a design. For example, the spontaneous removal may be possible without any nano-tier roughness.³⁵ Further work is needed to optimize the surface texture to promote the self-propelled sweeping removal toward the ultimate goal of enhancing dropwise condensation.

This work was supported by the National Science Foundation (CBET-12-36373) and the Department of Energy (CNMS-2012-094 and CNMS-2014-074). J.J.F. was supported by the Natural Sciences and Engineering Research Council of Canada. A portion of this research was conducted at the Center for Nanophase Materials Sciences, which is a DOE Office of Science User Facility.

This manuscript has been authored by UT-Battelle, LLC under Contract No. DE-AC05-00OR22725 with the U.S. Department of Energy. The United States Government retains and the publisher, by accepting the article for publication, acknowledges that the United States Government retains a non-exclusive, paid-up, irrevocable, world-wide license to publish or reproduce the published

form of this manuscript, or allow others to do so, for United States Government purposes. The Department of Energy will provide public access to these results of federally sponsored research in accordance with the DOE Public Access Plan (<http://energy.gov/downloads/doe-public-access-plan>).

- ¹E. Schmidt, W. Schurig, and W. Sellschopp, *Tech. Mech. Thermodyn.* **1**, 53 (1930).
- ²J. W. Rose, *Proc. - Inst. Mech. Eng., Part A* **216**, 115 (2002).
- ³V. P. Carey, *Liquid-Vapor Phase-Change Phenomena*, 2nd ed. (Taylor & Francis, New York, 2008).
- ⁴C. G. L. Furmidge, *J. Colloid Sci.* **17**, 309 (1962).
- ⁵J. W. Rose, *Chem. Eng. Res. Des.* **82**, 419 (2004).
- ⁶S. S. Beaini and V. P. Carey, *J. Enhanced Heat Transfer* **20**, 33 (2013).
- ⁷R. Enright, N. Miljkovic, J. L. Alvarado, K. Kim, and J. W. Rose, *Nanoscale Microscale Thermophys. Eng.* **18**, 223 (2014).
- ⁸A. Steyer, P. Guenoun, and D. Beysens, *Phys. Rev. Lett.* **68**, 64 (1992).
- ⁹S. Daniel, M. K. Chaudhury, and J. C. Chen, *Science* **291**, 633 (2001).
- ¹⁰C. H. Chen, Q. Cai, C. Tsai, C. L. Chen, G. Xiong, Y. Yu, and Z. Ren, *Appl. Phys. Lett.* **90**, 173108 (2007).
- ¹¹X. Chen, J. Wu, R. Ma, M. Hua, N. Koratkar, S. Yao, and Z. Wang, *Adv. Funct. Mater.* **21**, 4617 (2011).
- ¹²D. M. Anderson, M. K. Gupta, A. A. Voevodin, C. N. Hunter, S. A. Putnam, V. V. Tsukruk, and A. G. Fedorov, *ACS Nano* **6**, 3262 (2012).
- ¹³K. Rykaczewski, A. T. Paxson, S. Anand, X. Chen, Z. Wang, and K. K. Varanasi, *Langmuir* **29**, 881 (2013).
- ¹⁴M. He, Q. Zhang, X. Zeng, D. Cui, J. Chen, H. Li, J. Wang, and Y. Song, *Adv. Mater.* **25**, 2291 (2013).
- ¹⁵J. Tian, J. Zhu, H.-Y. Guo, J. Li, X.-Q. Feng, and X. Gao, *J. Phys. Chem. Lett.* **5**, 2084 (2014).
- ¹⁶C. Liu, J. Ju, Y. Zheng, and L. Jiang, *ACS Nano* **8**, 1321 (2014).
- ¹⁷K. O. Zamuruyev, H. K. Bardaweel, C. J. Carron, N. J. Kenyon, O. Brand, J.-P. Delplanque, and C. E. Davis, *Langmuir* **30**, 10133 (2014).
- ¹⁸A. Ghosh, S. Beaini, B. J. Zhang, R. Ganguly, and C. M. Megaridis, *Langmuir* **30**, 13103 (2014).
- ¹⁹D. Torresin, M. K. Tiwari, D. Del Col, and D. Poulikakos, *Langmuir* **29**, 840 (2013).
- ²⁰S. Anand, A. T. Paxson, R. Dhiman, J. D. Smith, and K. K. Varanasi, *ACS Nano* **6**, 10122 (2012).
- ²¹M. Kollera and U. Grigull, *Heat Mass Transfer* **2**, 31 (1969).
- ²²J. B. Boreyko and C. H. Chen, *Phys. Rev. Lett.* **103**, 184501 (2009).
- ²³N. Miljkovic and E. N. Wang, *MRS Bull.* **38**, 397 (2013).
- ²⁴N. Miljkovic, R. Enright, and E. N. Wang, *ACS Nano* **6**, 1776 (2012).
- ²⁵N. Miljkovic, R. Enright, Y. Nam, K. Lopez, N. Dou, J. Sack, and E. N. Wang, *Nano Lett.* **13**, 179 (2013).
- ²⁶J. B. Boreyko and C. H. Chen, *Int. J. Heat Mass Transfer* **61**, 409 (2013).
- ²⁷F. Liu, G. Ghigliotti, J. J. Feng, and C. H. Chen, *J. Fluid Mech.* **752**, 39 (2014).
- ²⁸F. Liu, G. Ghigliotti, J. J. Feng, and C. H. Chen, *J. Fluid Mech.* **752**, 22 (2014).
- ²⁹For non-wetting surfaces, a higher departure velocity is expected on a cornered pillar compared to a flat substrate, regardless of the bottom substrate. In the absence of the bottom substrate, i.e., on a long pillar, the coalescence-induced departure velocity is $v_d^* = 0.29$.
- ³⁰W. Vedder and D. A. Vermilyea, *Trans. Faraday Soc.* **65**, 561 (1969).
- ³¹M. He, X. Zhou, X. Zeng, D. Cui, Q. Zhang, J. Chen, H. Li, J. Wang, Z. Cao, Y. Song, and L. Jiang, *Soft Matter* **8**, 6680 (2012).
- ³²The substrate in Fig. 3 was subjected to ambient environments with various humidities and also room-temperature nitrogen stream saturated with water vapor by bubbling. The qualitative observations remained the same for both the nucleation process and the sweeping removal. A more comprehensive study is needed to explore the effects of supersaturation and noncondensable gases for different surface textures.
- ³³B. K. Chakraverty and G. M. Pound, *Acta Metall.* **12**, 851 (1964).
- ³⁴K. K. Varanasi, M. Hsu, N. Bhate, W. Yang, and T. Deng, *Appl. Phys. Lett.* **95**, 094101 (2009).
- ³⁵K. Zhang, F. Liu, A. J. Williams, X. Qu, J. J. Feng, and C. H. Chen, "Self-propelled droplet removal from fiber-based coalescers," *Phys. Rev. Lett.* (submitted).